CYCLIC QUASI-STATIC TESTING OF A HALF-SCALE, TWO-STORY UNREINFORCED MASONRY BUILDING WITH STRUCTURAL IRREGULARITY



Abide Aşıkoğlu
PhD Student
ISISE, University of Minho
Guimarães
abideasikoglu@hotmail.com

Graça Vasconcelos
Associate Professor
ISISE, University of Minho
Guimarães
graca@civil.uminho.pt

Paulo B. Lourenço
Full Professor
ISISE, University of Minho
Guimarães
pbl@civil.uminho.pt

ABSTRACT

Pushover analysis is a straightforward tool to be applied in engineering practice to validate a numerical method, or to use performance-based design/assessment methods. Yet, a limited number of the experimental campaign, which studies the building response in a quasi-static regimen, exists. In the present study, cyclic quasi-static testing of a half-scale two-story unreinforced masonry building with structural irregularity has been performed at the Laboratory of the Structures at the University of Minho. A typical building typology has been selected and the structural irregularity is introduced by a setback in one corner of the building plan. The loading has been applied as unidirectional at the centre of mass to observe the torsional effects due to irregularity. In the present paper, the testing procedure, and the main experimental findings are presented and discussed.

Keywords: Quasi-static test, cyclic, experimental pushover, unreinforced masonry, structural irregularities.

1. INTRODUCTION

Masonry is a versatile construction material that is used for structural and non-structural purposes. As a building material, it has various advantages. It is cost-effective, highly durable, and fire-resistant. It is a sustainable material, and recyclable. Unreinforced masonry (URM) buildings have exceptional insulation performance and so provide a comfortable indoor atmosphere even in hot countries. Moreover, URM buildings have timeless aesthetics. Most of the existing and heritage structures observed across the world are derivatives of URM. The construction of URM buildings is common in countries with low seismicity, such as the United Kingdom, Germany and Brazil [1]. Most often, URM buildings are found in low- to mid-rise residential or commercial structures (Figure 1). On the other hand, in most countries where the seismic activity is brutal, alternative construction materials, such as reinforced concrete and steel, have been favoured, and masonry has become a non-structural component. The main reason is URM structures are widely recognized to be particularly vulnerable to seismic events. Nevertheless, a significant portion of the building stock all around the world is composed of URM buildings and, still, URM is a competitive and promising construction solution. Yet, it is observed that URM buildings are relatively underdeveloped in seismic design regulations compared to other typologies. Further research and developments are essential to learn and improve the seismic response of these structures. Indeed, experimental studies are a crucial part of the research.

Figure 1. Examples of low- and mid-rise URM building construction [2]

The current study intends to provide experimental data at the structural level that may be used with greater confidence in numerical simulations, assessment of methodologies, and as well as to provide straightforward rules for implementing a technique to be used in practice. In this study, the experimental campaign includes (i) material characterization of masonry [3] (ii) quasi-static testing of a half-scale building, (iii) dynamic identification of the experimental building, and (iv) digital image correlation. This paper only addresses the part related to quasi-static testing.

At the Laboratory of the Structures at the University of Minho, cyclic quasi-static testing of a half-scale two-story unreinforced masonry building with structural irregularity was performed. A typical building typology was chosen (similar to Avila et al., 2018 [4]), and the structural irregularity was introduced by a setback in one corner of the building plan. The lateral load was applied at the centre of mass as cyclic unidirectional. The present paper discusses a review of prior experimental campaigns, the design of the experimental setup and the testing procedure. The key experimental results are given and analyzed.

2. PREVIOUS EXPERIMENTAL STUDIES

The execution of experimental campaigns aimed at replicating the seismic response is an expensive and demanding process. There are numerous constraints to performing a test on a building scale, such as the number of experimental models, available equipment, budgetary concerns, limited time, and expertise. It is observed that there are few experimental tests on URM buildings that are based on quasi-static loading (Figure 2). Due to its complexity, pseudo-dynamic tests of URM buildings are uncommon (Figure 3), however, a large variety of shaking table tests are available in the literature (Figure 4). It is highlighted that the majority of the experimental campaigns were designed to investigate the seismic response of historical and existing URM structures mainly with timber floors or without any slab systems. On the other hand, only a few research groups studied modern URM buildings with reinforced concrete slabs [4]–[6]. In the case of modern URM, innovative structural solutions have been pursued to improve the seismic performance of these structures to restore their attractiveness.

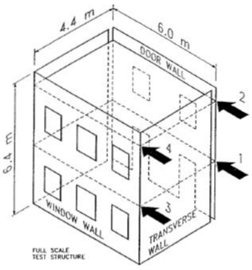

[7]

[8]

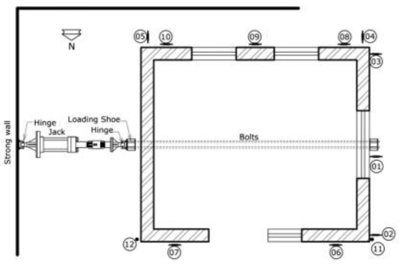

[5]

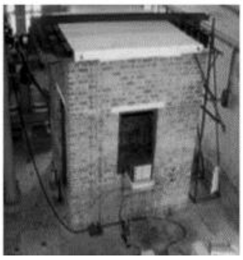

[6]

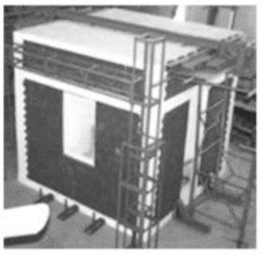

[6]

[9]

Figure 2. Different experimental setups of quasi-static testing

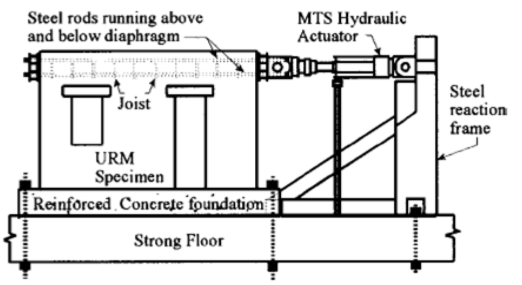

[10]

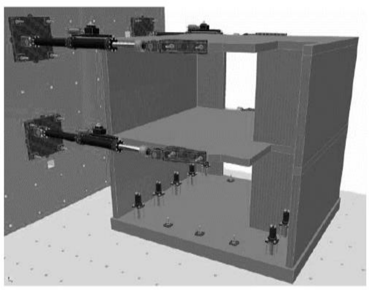

[11]

Figure 3. Examples of pseudo-dynamic test applications

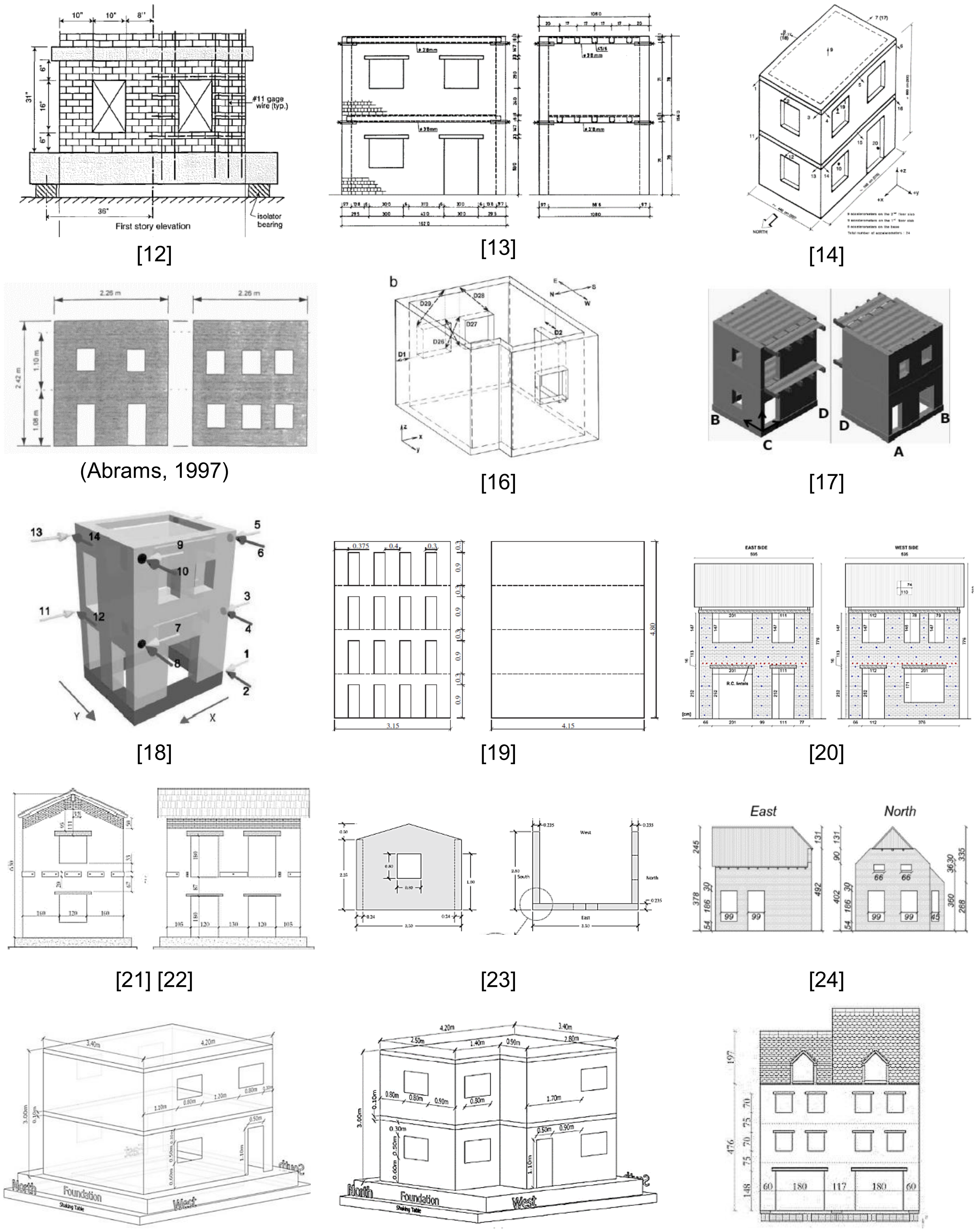

Figure 4. Different structural configurations tested on shaking table

3. EXPERIMENTAL SETUP

The experimental model was designed to represent typical residential Portuguese houses which are commonly characterized by a structurally irregular layout due to architectural, economical, and functional concerns. The design covers Eurocode 8 (2004) [28] criteria for (i) bi-directional resistance and stiffness, (ii) torsional resistance and stiffness, and (iii) diaphragm behaviour of the slabs. The experimental building is irregular in the plan which has a setback on one side. The geometry of the building was chosen based on the experimental model tested by Avila et al. (2018).

The half-scale two-story URM building has a plan dimension of 419 cm x 368 cm with an inter-story height of 152 cm, as shown in Figure 5. The box behaviour is ensured by a reinforced concrete slab, which has a 10 cm thickness. The building was composed of vertical perforated clay masonry brick units which are available in the market. The masonry arrangement was decided as a running bond with the interlocking of the intersecting orthogonal walls. The dimensions of clay masonry brick units are 24.5 cm x 10.8 cm x 9.8 cm. As per Eurocode 6 (2018) [29], the clay masonry brick unit is classified as Group 3 having a compressive strength of a minimum of 15 MPa. Class M10 ready-mixed mortar is chosen for bed joints and head joints.

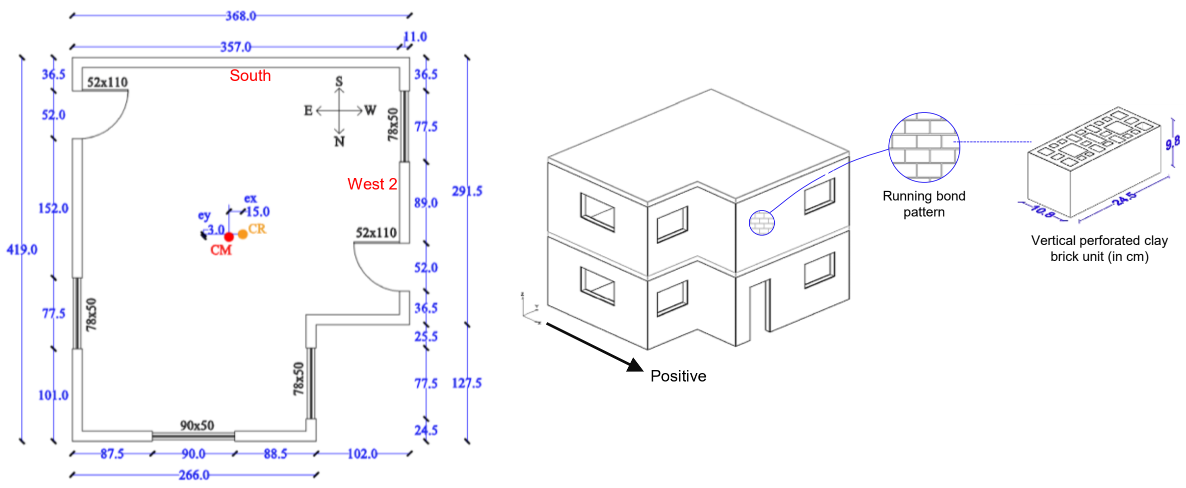

Figure 5. Geometric details and axonometric view of the experimental building

During the design and construction of the experimental building, it was observed that the dimension of the brick units was an important parameter regarding the practical application. One of the criteria during the selection process of the brick units was the representativeness of half-scale units due to scaled building. Meaning that, if the length over width ratio of the brick unit is equal to 2, then it provides easier application. In the present case, this ratio was nearly 2.3 and, therefore, during the construction of the walls, the location of each brick should be done correctly according to the design (Figure 6). Otherwise, a random distribution of such bricks may result in the length of walls that were not in the design.

The design of the experimental setup is mainly controlled by the application of the loading. In other words, two hydraulic jacks with a capacity of 300 kN were installed to apply the lateral loading at each level. They were located at the centre of mass of the structure at the floor levels. To avoid point load application, steel profiles along the perimeter of the building were mounted as demonstrated in Figure 7.

Figure 6. Construction of the URM walls

Figure 7. Construction progress of the RC slab

Another important feature of this experimental campaign is the use of post-tensioned rebars with a diameter of 20 mm which were located inside the RC slab as a non-structural component. Otherwise, the post-tensioned bars should have been located below or above the slab through holes that would be made or left on the structural walls. To avoid any damage prior to the testing or concentration of any deformation, the first approach was adopted. It is highlighted that these post-tensioned rebars were placed inside PVC tubes with a diameter of 24 mm to avoid them to harden with concrete and to provide free movement before the post-stressing. The main aim of such application was to ensure the integrity of the steel profiles during the pulling and pushing of the structure and to avoid the detachment of the profiles from the slab so that they could distribute the load uniformly. Moreover, the steel profiles were used as a framework for the slab and cast with concrete to safeguard complete coverage of theinterface between the RC slab and the steel profiles.

Figure 8. Details of the RC slab with post-tensioned rebars and their connection

Accordingly, the section view of the setup details is provided in Figure 9. Each hydraulic jack was installed on a reaction wall and the load application point of the jacks was connected to steel plates which were fixed to the loading beams, as shown in Figure 10(a). In this paper, these plates are called loading plates (Figure 10(b)). To apply the cyclic load, the structure was pushed and pulled through these connections. On the same alignment at the opposite wall, so-called reloading plates were mounted (Figure 10(c)). Loading and reloading plates were fixed to each other through the post-tensioned rebars. In this way, the force was transferred to the opposite wall to represent the loading in the negative direction during the reloading and pulling phase. The final configuration of the experimental setup at the time of testing is shown in Figure 11.

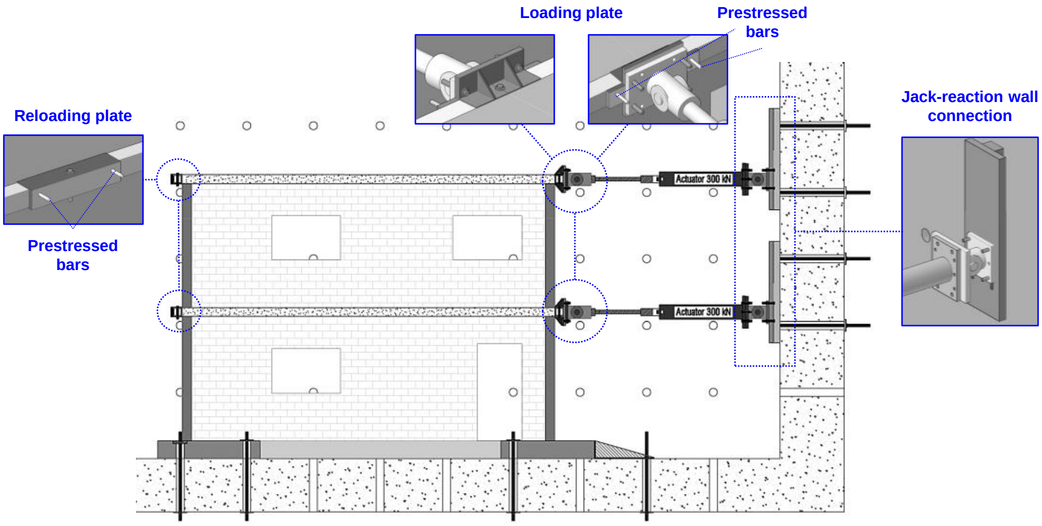

Figure 9. Configuration and details of the experimental setup, section view

(a) (b) (c)

Figure 10. Configuration of the loading instrumentation, (a) hydraulic jacks located at the centre of mass, (b) loading plate detail, (c) reloading plate detail

Figure 11. Views from the experimental building at the testing condition

As part of the development of the experimental setup, the instrumentation was designed to get the most relevant and important measurement to evaluate the performance during the test. In this regard, a set of Linear Variable Differential Transformers (LVDT) was placed at the different locations of the building to obtain local and global deformations as depicted in Figure 12. With this aim, a total number of 39 LVDTs were installed and they were categorized into four groups to measure (i) shear (16), (ii) lateral (17), (iii) uplift (3), and (iv) sliding (3) deformations. At the piers where shear failure was expected, the diagonal configuration was implemented for 16 LVDTs. On the other hand, 17 LVDTs were installed to measure the global lateral displacement of the building at the corners and the middle of the walls as in-plane and out-of-plane deformations. Furthermore, 3 LVDTs were mounted to measure the sliding deformations at the base of the walls and foundation in the front façade only to check if there is any movement even though it was not expected. Lastly, at the locations where the rocking/crushing response might be relevant, 3 LVDTs were placed.

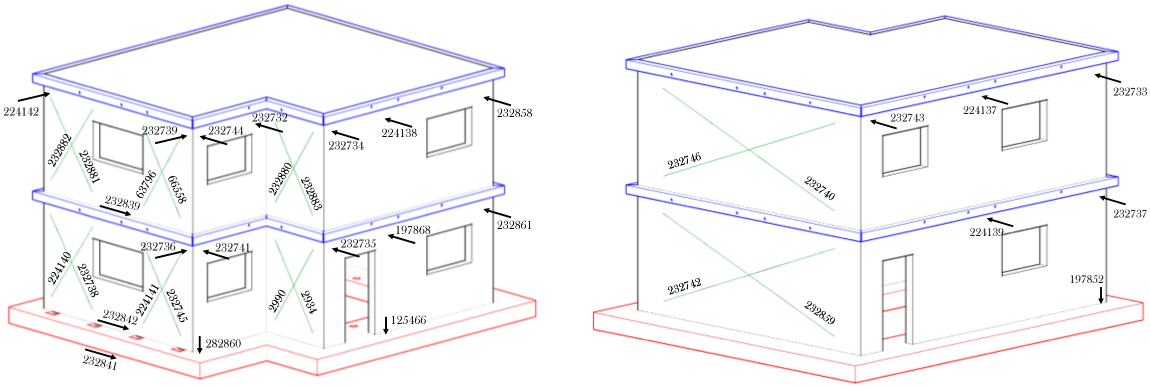

Figure 12. Configuration of the LVDT equipment

4. LOADING PROTOCOL

The test structure was subjected to a sequence of load cycles in which the forces at the floor level were gradually increased. It was decided to apply the loading in force-control because the capacity of the structure was unknown although there was a preliminary analysis, and the building was significantly sensitive to low levels of displacements. Each cycle consisted of a load pattern that was selected based on the first dominant mode shape of the building in the transversal direction. Accordingly, the loading protocol was derived based on the two-step simplification. The first step considers the conversion of the building as a multi-degree-of-freedom (MDOF) system to a single-degree-of-freedom (SDOF) system through the period of the structure obtained from the dynamic identification (Figure 13). By using the simple relation of the period (Equation 1), it is possible to calculate the equivalent stiffness of the SDOF system since the equivalent mass is known.

$$T = 2\pi\sqrt{\frac{m}{k}} \tag{1}$$

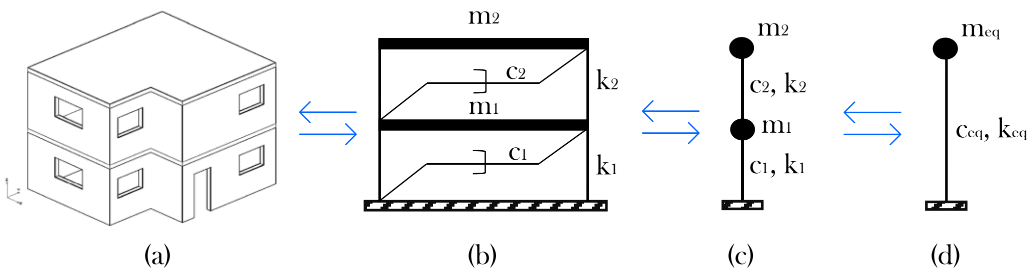

Figure 13. Substitute structural approach, (a) detailed structure, (b) simplified model, (c) 2 DOFs system, (d) SDOF system

In the second step, it is assumed that 2 degree-of-freedom (DOF) system can be acquired from the SDOF system being the equivalent stiffness is the equivalence of two springs connected in series. Therefore, the stiffness at each level was computed by assuming the stiffness and mass at each DOF was equal and the stiffness and mass matrix for the 2 DOF system is obtained. Then, the eigenvalue analysis was computed for the 2 DOF system and the eigenvectors were obtained. The normalized eigenvectors were used to define the load pattern. It was found that the structure should be subjected to 1 unit of force at the top level while in the first level 0.6 unit of force was needed. At each cycle, the same relation was used. Figure 14 presents the loading protocol that was used for the cyclic quasi-static test in terms of total base shear force and base shear coefficient (BSC, relation to the total weight of the structure). At the beginning of the test, the loading pattern was applied in displacement-control however it was not possible to ensure the relation of the forces. Thus, force-control was implemented in the testing procedure. The loading protocol is gathered in Table 1. The table starts from Cycle 3 because the first two cycles were performed in displacement-control and decided to be neglected due to the reason mentioned above. Due to limitations of the equipment, the loading at each level was applied step-wise, meaning that one level was subjected at a time.

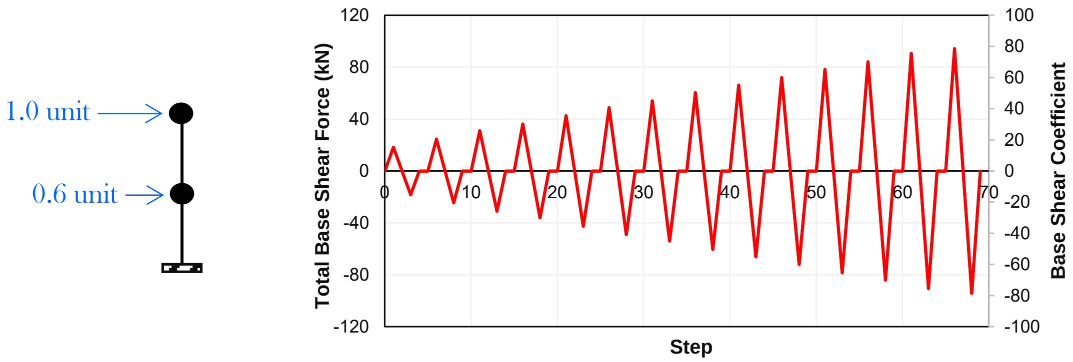

Figure 14. Applied loading protocol in force control

Table 1. Load protocol

Cycle	Force (kN)	BSC (%)
3	18.24	15
4	24.64	21
5	31.04	26
6	36.16	30
7	42.56	35
8	48.96	41
9	54.08	45
10	60.48	50
11	66.24	55
12	72.00	60
13	78.40	65
14	84.16	70
15	90.56	75
16	93.6	78

5. RESULTS

The results are discussed qualitatively and quantitatively such as (i) evolution of the damage, (ii) capacity diagram, and (iii) displacement profiles along the height in the in-plane and out-of-plane walls. First of all, the lateral capacity of the building is assessed in terms of base shear and lateral displacement response. The base shear coefficient was computed as the ratio of the total base shear force and the total weight of the structure. On the other hand, the drift which is the ratio of the top displacement and the height of the building is considered. The capacity diagrams for each cycle and the backbone curve are provided in Figure 15. To plot the capacity diagrams, LVDTs right below the reloading plates were selected at each level. It is found that in terms of lateral load capacity the structure has a similar level of load in both positive and negative directions which was 75% of the total structural weight (nearly 90 kN). In addition, the displacements are significantly higher in the negative load direction which might be due to the uplifting of the structure in this direction (nearly 0.09%). On the other hand, the maximum drift was achieved at the 0.05% in the positive direction. It is noted that the test was performed up to the maximum lateral load capacity of the building, once the failure was reached since the loading was applied in force-control. Therefore, the post-peak behaviour was not achieved.

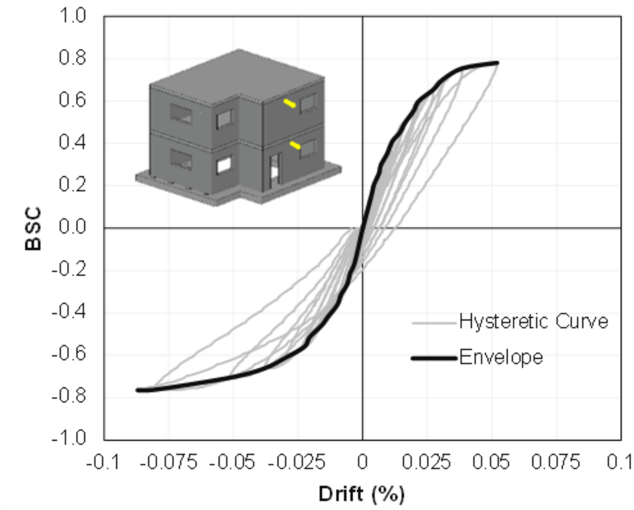

Figure 15. Capacity diagram for a given control point

In the negative phase of Cycle 13 (which is 65% of the total weight) uplifting of the walls from the foundation and slab was noticed at the first and second levels, respectively. The uplift occurred at the base of the west and south wall. As the load was increased, the level of uplift got higher and finally reached the maximum at the peak of Cycle 15 (75% of the weight). In Figure 16, the results of Cycle 16 represent the failure and, therefore, displacements after 0.5 mm are constant. In other words, Cycle 16 (78% of the weight) was ended as the repetition of Cycle 15.

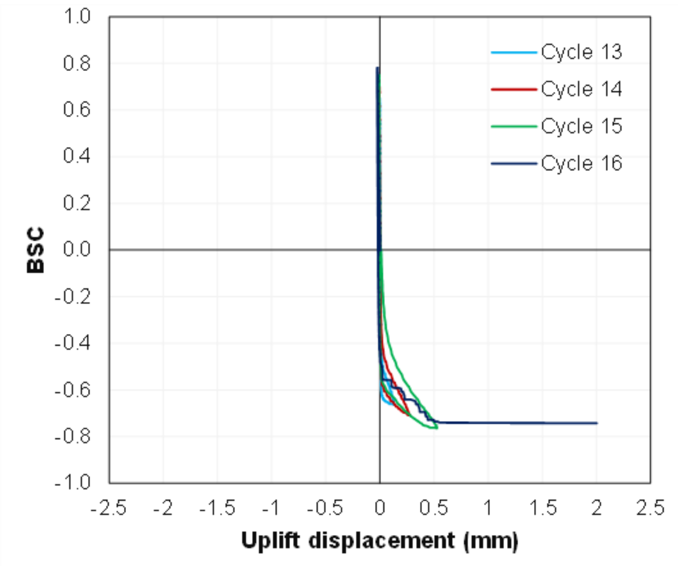

Figure 16 BSC vs displacement diagram of the uplift

The in-plane drift profiles along the height of the building corresponding to each cycle are presented in Figure 17 and Figure 18, for out-of-plane and in-plane drifts, respectively. It is found that in-plane drifts corresponding to the negative load direction are significantly higher than the positive one during the last few cycles. The maximum top drift was found as nearly 0.05% under the lateral loading in the positive direction while a drift of 0.09% was recorded for the negative direction.

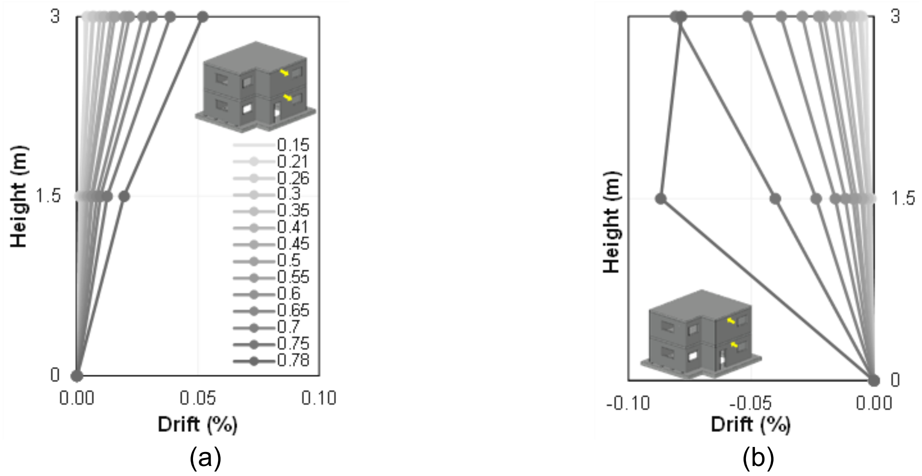

Figure 17 Out-of-plane total drift profiles in the (a) positive, (b) negative direction

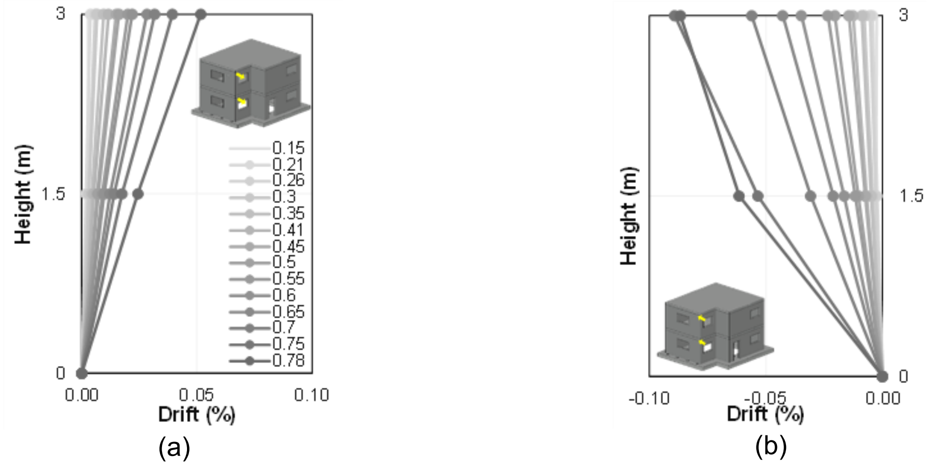

Figure 18 In-plane total drift profiles in the (a) positive, (b) negative direction

Inter-story drift ratio is a good damage indicator since the relative displacements of adjacent floors impose the damage. It provides an idea of the distribution of the deformations. In the present case, it is observed that higher deformations were recorded and concentrated in the second level both in the positive and negative direction. Inter-story drift ratio in the negative direction is higher than the in-plan drift ratio at the top of the building (being nearly 0.12%)

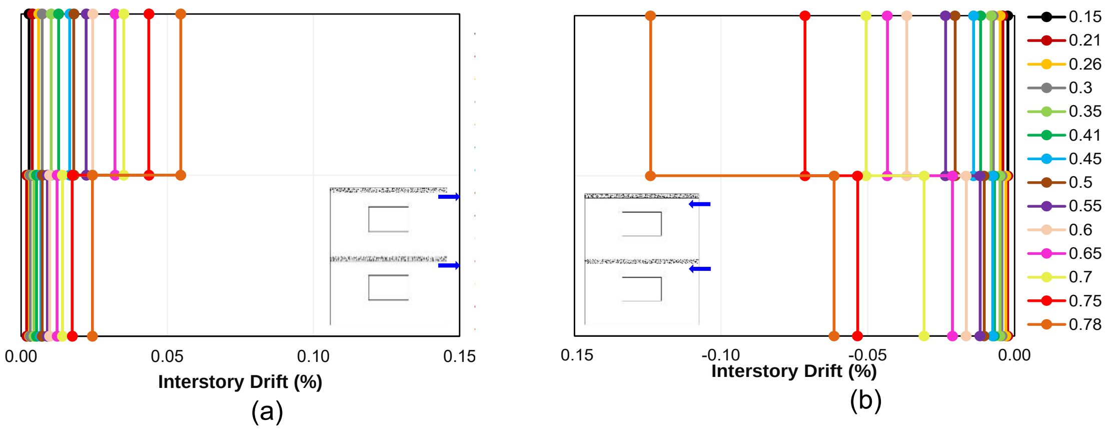

Figure 19 Inter-story drift ratio along the height of the North façade in the (a) positive, (b) negative direction

The evolution of the damage and crack patterns of the experimental building that was visible is shown in Figure 20. The red colour indicates the cracks due to loading in the positive direction while blue represents the cracks resulting from loading in the negative direction. The crack was initiated when the lateral load reached 60% of the total weight of the structure. The first cracks were observed in the pier of the front (north façade) as sort of flexural. Additionally, horizontal cracks in the out-of-plane direction walls were also noted (Figure 20(a)). By increasing the load by 5%, the flexural cracks were extended, and additional horizontal cracks appeared at the region of the setback (Figure 20(b)). The appearance of the horizontal cracks might be associated with the torsional influence. Accordingly, the uplift started to dominate the response under the lateral loading in the negative direction once the lateral load exceeds 70% of the total weight as highlighted in blue in Figure 20(c). At the end of the experiment, the structural walls were severely detached from the foundation on the first floor and the slab on the second floor (Figure 21). Furthermore, moderate diagonal cracks were also noted. Yet, the structural response was mainly governed by the uplifting of the complete structure. Therefore, the structural walls were not able to contribute to energy dissipation throughout the building.

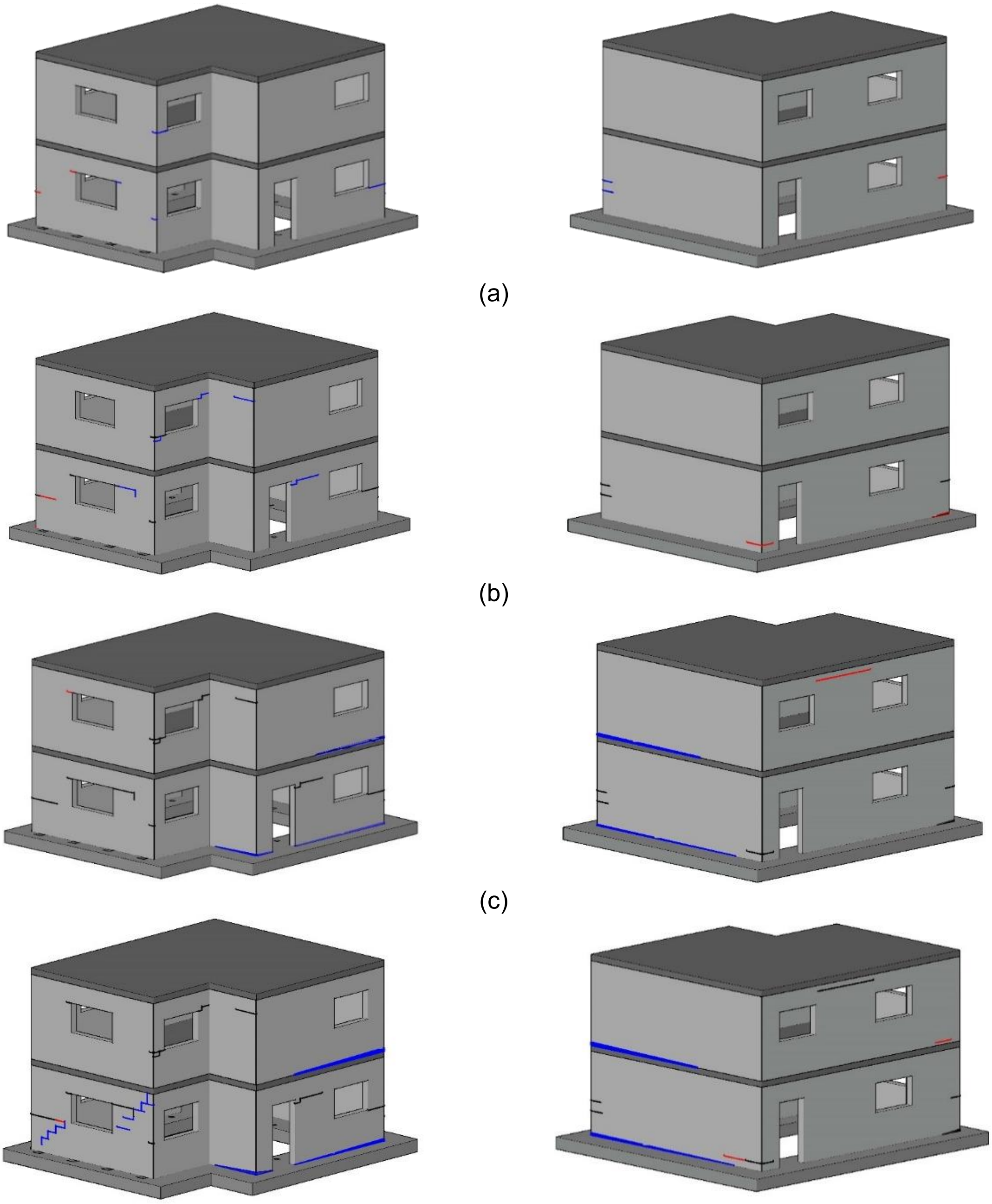

(a)

(b)

(c)

(d)

Figure 20 Crack evolution during the test at the end of (a) Cycle 12, (b) Cycle 13, (c) Cycle 14, (d) Cycle 15

Figure 21 Uplift at the base of the URM walls at Cycle 15 (Base shear force is equal to 75% of the total weight)

6. CONCLUSIONS

The present paper discusses an application of a cyclic quasi-static test on a half-scale two-story unreinforced masonry building with a plan irregularity. A brief literature review was presented to emphasize the need for such a study. It is noted that the design and construction of an experimental setup require comprehensive planning, and a set of unique features are described in this paper. Accordingly, the methodology behind the application of the loading was explained. Due to a few limitations of the equipment, the load application was carried out in force-control in a stepwise scheme, meaning that loading of the two jacks was not applied simultaneously and it was employed through one hydraulic jack at a time. Based on the observations during the test, the experimental setup worked well and uniform distribution of the loading during pushing and pulling was ensured utilizing steel beams and the post-tensioned tie-rods. The crack initiation was observed at the piers in the front (north) façade of the building as flexural cracks. A set of horizontal cracks which might be associated with the torsional effect were noticed. The structure reach failure at 75% of the total weight of structure which was mainly governed by the rocking of the complete building. Although the results are representations of half-scale building, comparing with a full-scale building, a significant difference in terms of base shear coefficient and inter-story drift ratio is not expected despite of the fact that the displacements and force required for a full-scale building is considerably higher than the half-scale one. As a future task, it is decided to repair the horizontal cracks at the base of the walls and apply additional mass on both slabs then repeat the test with the same approach.

ACKNOWLEDGEMENTS

This work is financed by national funds through FCT - Foundation for Science and Technology, under grant agreement SFRH/BD/143949/2019 attributed to the 1st author. Additionally, this work is financed by national funds through FCT - National Foundation for Science and Technology, in the scope of the research project “Experimental and Numerical Pushover Analysis of Masonry Buildings (PUMA)” (PTDC/ECI-EGC/29010/2017).

REFERENCES

[1] P. . Lourenço and R. Marques – "Design of masonry structures (General rules): Highlights of the new European masonry code", in *Brick and Block Masonry - From Historical to Sustainable Masonry*, Kubica, Kwiecien, and Bednarz, Eds. Krakow: Taylor & Francis, 2020.

[2] K. Beyer, M. Tondelli, F. Vanin, S. Petry, and A. Paparo – "Seismic behaviour of unreinforced masonry buildings with reinforced concrete slabs: Assessment of in-plane and out-of-plane response", 2015. [Online]. Available: https://www.bafu.admin.ch/dam/bafu/en/dokumente/erdbeben/externe-studien-berichte/seismic_behaviorofunreinforcedmasonrybuildingswithreinforcedconcreteslabs.pdf.download.pdf/seismic_behaviourofunreinforcedmasonrybuildingswithreinforcedconcreteslabs.pdf.

[3] A. Aşıkoğlu, A. Del Re, G. Vasconcelos, and P. B. Lourenço – "Quasi-Static Test on a Half-Scale Two-Story Urm Building : Quasi-Static Test on a Half-Scale Two-Story Urm Building : Mechanical Chracterization of", in *12th National Congress on Experimental Mechanics*, 2021, p. 1–14.

[4] L. Avila, G. Vasconcelos, and P. B. Lourenço – "Experimental seismic performance assessment of asymmetric masonry buildings", *Eng. Struct.*, 2017, vol. 155, no., p. 298–314, 2018, doi: 10.1016/j.engstruct.2017.10.059.

[5] K. Shahzada *et al.* – "Experimental seismic performance evaluation of unreinforced brick masonry buildings", *Earthq. Spectra*, vol. 28, no. 3, p. 1269–1290, 2012, doi: 10.1193/1.4000073.

[6] A. Chourasia, S. K. Bhattacharyya, N. M. Bhandari, and P. Bhargava – "Seismic Performance of Different Masonry Buildings: Full-Scale Experimental Study", *J. Perform. Constr. Facil.*, 2016, vol. 30, no. 5, p. 04016006, , doi: 10.1061/(ASCE)CF.

[7] G. Magenes, G. M. Calvi, and G. Kingsley – "Seismic Testing of a Full-scale, Two-story Masonry Building: Test Procedure and Measured Experimental Response", 1995. [Online]. Available: http://scholar.google.com/scholar?hl=en&btnG=Search&q=intitle:Seismic+testing+of+a+full-scale,+two-story+masonry+building:+Test+procedure+and+measured+experimental+response#0.

[8] A. Aldemir, B. Binici, E. Canbay, and A. Yakut – "Lateral load testing of an existing two story masonry building up to near collapse", *Bull. Earthq. Eng.*, 2017, vol. 15, no. 8, p. 3365–3383, doi: 10.1007/s10518-015-9821-3.

[9] A. Aldemir, B. Binici, E. Canbay, and A. Yakut – "In Situ Lateral Load Testing of a Two-Story Solid Clay Brick Masonry Building", *J. Perform. Constr. Facil.*, 2018, vol. 32, no. 5, p. 04018058, doi: 10.1061/(asce)cf.1943-5509.0001206.

[10] J. Paquette and M. Bruneau – "Pseudo-Dynamic Testing of Unreinforced Masonry Building with Flexible Diaphragm", *J. Struct. Eng.*, 2003, vol. 129, no. 6, p. 708–716, doi: 10.1061/(asce)0733-9445(2003)129:6(708).

[11] A. Anthoine and F. J. Molina – "Pseudo-dynamic testing of full scale masonry structures: Preparatory work", 2008.

[12] T. J. Paulson, D. P. Abrams, and R. L. Mayes – "Shaking-table study of base isolation for masonry buildings", *J. Struct. Eng. New York, N.Y.*, 1991, vol. 117, no. 11, p. 3315.

[13] M. Tomaževič, M. Lutman, and P. Weiss – "Seismic Upgrading of Old Brick-Masonry Urban Houses: Tying of Walls with Steel Ties", *Earthq. Spectra*, 1996, vol. 12, no. 3.

[14] D. Benedetti, P. Carydis, and P. Pezzoli – "Shaking table tests on 24 simple masonry buildings", *Earthq. Eng. Struct. Dyn.*, 1998, vol. 27, no. 1, p. 67–90.

[15] D. P. Abrams – "Response of unreinforced masonry buildings", *J. Earthq. Eng.*, 1997, vol. 1, no. 1, p. 257–273, doi: 10.1080/13632469708962368.

[16] R. Bairrão and M. J. F. Silva – "Shaking table tests of two different reinforcement techniques using polymeric grids on an asymmetric limestone full-scaled structure", *Eng. Struct.*, 2009, vol. 31, no. 6, p. 1321–1330, doi: 10.1016/j.engstruct.2008.04.039.

[17] M. Dolce *et al.* – “3D Dynamic Tests on 2 / 3 Scale Masonry Buildings Retrofitted With Different Systems”, *Proc. 14th World Conf. Earthq. Eng.*, 2008.

[18] N. Mazzon *et al.* – “Shaking Table Tests on Two Multi-leaf Stone Masonry Buildings”, *11th Can. Mason. Symp.*, 2009.

[19] N. Mendes – “Seismic Assessment of Ancient Masonry Buildings : Shaking Table Tests and Numerical Analysis”, University of Minho, 2012.

[20] F. Graziotti, U. Tomassetti, S. Kallioras, A. Penna, and G. Magenes – “Shaking table test on a full scale URM cavity wall building”, *Bull. Earthq. Eng.*, 2017, vol. 15, no. 12, p. 5329–5364, doi: 10.1007/s10518-017-0185-8.

[21] G. Magenes, A. Penna, I. E. Senaldi, M. Rota, and A. Galasco – “Shaking table test of a strengthened full-scale stone masonry building with flexible diaphragms”, *Int. J. Archit. Herit.*, 2014, vol. 8, no. 3, p. 349–375, doi: 10.1080/15583058.2013.826299.

[22] I. Senaldi, G. Magenes, A. Penna, A. Galasco, and M. Rota – “The effect of stiffened floor and roof diaphragms on the experimental seismic response of a full-scale unreinforced stone masonry building”, *J. Earthq. Eng.*, 2014, vol. 18, no. 3, p. 407–443, doi: 10.1080/13632469.2013.876946.

[23] P. X. Candeias, A. Campos Costa, N. Mendes, A. A. Costa, and P. B. Lourenço – “Experimental Assessment of the Out-of-Plane Performance of Masonry Buildings Through Shaking Table Tests”, *Int. J. Archit. Herit.*, 2017, vol. 11, no. 1, pp. 31–58, doi: 10.1080/15583058.2016.1238975.

[24] S. Kallioras *et al.* – “Experimental seismic performance of a full-scale unreinforced clay-masonry building with flexible timber diaphragms”, *Eng. Struct.*, 2018, vol. 161, no. January, p. 231–249, doi: 10.1016/j.engstruct.2018.02.016.

[25] P. B. Lourenço, L. Avila, G. Vasconcelos, J. P. P. P. Alves, N. Mendes, and A. C. Costa – “Experimental investigation on the seismic performance of masonry buildings using shaking table testing”, *Bull. Earthq. Eng.*, 2013, vol. 11, no. 4, p. 1157–1190, doi: 10.1007/s10518-012-9410-7.

[26] G. Guerrini *et al.* – “Experimental and Numerical Assessment of the Seismic Performance of a Half-Scale Stone Masonry Building Aggregate”, *16th Eur. Conf. Earthq. Eng.*, no. June 2018, pp. 1–12, 2018.

[27] I. E. Senaldi *et al.* – “Experimental seismic performance of a half-scale stone masonry building aggregate”, *Bull. Earthq. Eng.*, no. May, 2019, doi: 10.1007/s10518-019-00631-2.

[28] Eurocode 8, “EN 1998-1: Design of structures for earthquake resistance - Part 1: General rules, seismic actions and rules for buildings”, 2004.

[29] Eurocode 6, *Eurocode 6 - Design of masonry structures - Part 1-1: General rules for reinforced and unreinforced masonry structures*. 2018.